also be correct for a metal with superconducting fluctuations and it might be experimentally favorable to search for fluctuation effects in the far infrared near the peaks of the phonon density of states instead of at low frequencies.

The author would like to thank Professor A. J. Sievers and Mr. D. G. B. Tanner for many helpful discussions and reading the draft of this paper, and Professor V. Ambegaokar and Dr. A. B. Bringer, Dr. B. R. Patton, and Dr. K. W. Kehr for discussions concerning the Kramers-Kronig relations.

*Work supported by the U. S. Atomic Energy Commission under contract No. AT(30-1)-2391. Additional support was received from the Advanced Research Projects Agency through the Materials Science Center at Cornell University.

[1]D. C. Mattis and J. Bardeen, Phys. Rev. 111, 412 (1958).

[2]M. Tinkham, in *Optical Properties and Electronic Structure of Metals and Alloys*, edited by F. Abeles (North-Holland, Amsterdam, 1966), p. 431.

[3]R. R. Joyce and P. L. Richards, Phys. Rev. Lett. 24, 1007 (1970).

[4]T. Holstein, Phys. Rev. 96, 535 (1954).

[5]H. D. Drew and A. J. Sievers, Phys. Rev. Lett. 19, 697 (1967).

[6]G. Brändli and A. J. Sievers, to be published.

[7]Supplied by G. C. Adams from E. I. duPont de Nemours and Co., Film Department, Wilmington, Dela.

[8]This small temperature change does not noticeably increase the dc conductivity of the Pb, and it does not affect the properties of the polyethylene spacing material.

[9]A. Gavini and T. Timusk, Phys. Rev. B 3, 1049 (1971).

[10]P. B. Allen, Phys. Rev. B 3, 305 (1971).

[11]W. Shaw and J. C. Swihart, Bull. Amer. Phys. Soc. 16, 352 (1971).

[12]S. B. Nam, Phys. Rev. 156, 470, 487 (1967).

[13]J. M. Rowell, W. L. McMillan, and P. W. Anderson, Phys. Rev. Lett. 14, 633 (1965). The impurity band found by these authors is not detectable in the present data.

[14]A. B. Pippard, in *Low Temperature Physics*, edited by C. DeWitt, B. Dreyfus, and P. G. deGennes (Gordon and Breach, New York, 1962), p. 58.

[15]R. A. Ferrell and R. E. Glover, Phys. Rev. 109, 1398 (1958).

[16]H. Scher, Phys. Rev. Lett. 25, 759 (1970), and Phys. Rev. B 3, 3551 (1971).

Near-Resonance Spin-Flip Raman Scattering in Indium Antimonide

S. R. J. Brueck and A. Mooradian

Lincoln Laboratory, Massachusetts Institute of Technology, Lexington, Massachusetts 02173

(Received 25 October 1971)

Using a discretely tunable CO laser, we have studied the resonance enhancement of spontaneous spin-flip Raman scattering together with its polarization selection rules. Good agreement is found between experiment and theory.

We report here a study of spontaneous Raman scattering from electron spin-flip excitations in indium antimonide for laser pump frequencies near band-gap resonance. Both the dependence of the relative resonance enhancement factor on the incident photon energy and the polarization selection rules are compared with theory.

A liquid-nitrogen–cooled CO laser was used to pump spontaneous spin-flip Raman scattering with an electron density of 1×10^{16} cm^{-3} in an InSb crystal that was mounted on a cold finger ($T\sim30$°K) in the bore of a superconducting magnet. The CO laser could be made to oscillate on any of a large number of closely spaced (2–4 cm^{-1}) lines between 5.0 and 6.1 μm by adjusting a grating which was used as one of the laser mirrors. Typical multimode laser output power was 3–4 W. A sapphire $\frac{1}{2}$-wave plate was used to control the polarization of the incident light. The scattered light was analyzed with a $\frac{1}{4}$-m spectrometer and KBr foreprism together with a Cu:Ge detector. A gold-wire grid polarizer of polarization ratio 1:400 was used in conjunction with a sapphire $\frac{1}{4}$-wave plate as an analyzer. The spectrometer wavelength and polarization response were calibrated using a Globar source.

The sample was mounted with an array of small mirrors so that the incident light could be directed either along or normal to the magnetic field $\vec{H}$, and the scattered light could be collected either along $\vec{H}$ or at right angles to $\vec{H}$ (both in the direction collinear with the incident light and at right angles to the incident light).

Figure 1 shows the polarization data obtained for a geometry in which the incident light propagated normal to the magnetic field ($\vec{k}_i\perp\vec{H}$), and

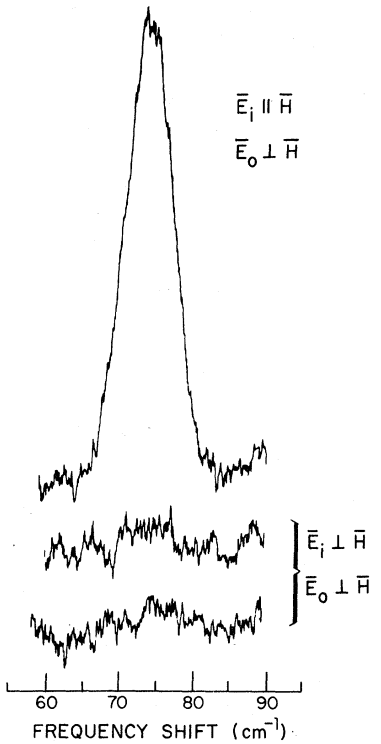

FIG. 1. Polarization of spin-flip Raman scattering. The incident photons are propagating normal to $\vec{H}$ and are polarized both along $\vec{H}$ (top trace) and normal to $\vec{H}$ (bottom traces). The scattered light is propagating along $\vec{H}$, and one linearly polarized component is collected in the top traces and the orthogonal component in the bottom trace. $n = 1\times10^{16}$ cm^{-3}, $H = 35$ kG, and $T \sim 30$°K.

the scattered light was collected along $\vec{H}$ ($\vec{k}_0 \parallel \vec{H}$). In the top trace, the incident photons were polarized along the magnetic field direction ($\vec{E}_i \parallel \vec{H}$), and one of the two orthogonal linear polarizations of the scattered light was collected. The bottom traces show the two orthogonal linear polarizations of the scattered light when the polarization of the incident beam is rotated by $\pi/2$ ($\vec{E}_i \perp \vec{H}$). The incident photon energy was 232.0 meV and the magnetic field strength was 35 kG. The scattered light was collected from a solid angle inside the sample of approximately 0.001 sr (this corresponds to an angular spread of ~1°) in order to avoid any depolarization effects due to too large a collection angle. The spectrometer slits were masked to ensure that no stray light, scattered from the edges of the sample, was collected.

A numerical calculation of the incident photon energy and the magnetic field dependence of the spin-flip Raman-scattering cross section was performed using the Pidgeon and Brown[1] model Hamiltonian to evaluate the InSb band structure. The calculation was similar to that described by Wright, Kelley, and Groves.[2] The results of this calculation are used in the comparison of theory and experiment given here.

For the purposes of a discussion of the results, an approximate analytic expression of the cross section can be obtained[3] by a calculation similar to those of Yafet[4] and Makharov,[5] in which the InSb band structure is evaluated to first order in the magnetic field strength. The experimental results reported here were all obtained for a magnetic field and electron concentration such that all conduction electrons were in the lower spin level of the $n = 0$ Landau level in thermal equilibrium. For the experimental situation of an incident photon energy very close to the InSb band-gap energy, the dominant physical mechanism in the scattering is a two-step process involving the virtual excitation of an electron from a valence-band state into the conduction-band upper spin level ($n = 0$ Landau level) with the absorption of an incident photon, followed by the virtual transition of an electron from the lower conduction-band spin level to the valence-band state with the emission of the scattered photon. The net change in the electronic states is simply the excitation of an electron from the lower to the higher, $n = 0$, conduction-band spin level. The largest contributions to the cross section occur via light-hole valence-band states of Landau-level number $n = -1$ and via heavy-hole valence-band states. In this simplified band model, in which free-mass terms and the interaction of the conduction and valence bands with higher bands have been neglected, the energies of these states are independent of magnetic field and are taken as the zero-energy reference. The expression for the cross section is

$$\frac{d\sigma}{d\Omega} = \left(\frac{e^2}{mc^2}\right)^2 \frac{\omega_0}{\omega_i}\left(\frac{mP^2}{3\hbar^2}\right)^2 \left| e_{iz}e_{0-}\,\frac{1-\frac{1}{3}a^2-\frac{1}{3}b^2+Aa}{E_{c,\beta}-\hbar\omega_i} - \frac{6}{7}e_{i+}e_{0z}\,\frac{1-\frac{2}{3}a^2-\frac{1}{3}b^2-Aa}{E_{c,\beta}-\hbar\omega_i}\right|^2, \tag{1}$$

where ω_i (ω_0) is the frequency and e_i (e_0) is the polarization of the incident (scattered) photon. The additional subscript on the polarization indicates the polarization components relative to the z-directed magnetic field, $e_\pm = e_x \pm ie_y$; $E_{c,\beta}$ is the energy of the conduction-band upper spin level, and P is the in-

terband matrix element (in eV cm). The terms in a, b, and A arise from the mixing of the conduction- and valence-band wave functions in a magnetic field. Here $a = P\sqrt{s}/E_g$, $b = P\sqrt{s}/(E_g + \Delta)$, and $A = (\hbar^4 s/m^2P^2)^{1/2}$, E_g being the band-gap energy, Δ the spin-orbit–split energy, and $\sqrt{s} = (eH/\hbar c)^{1/2}$ the inverse of the classical cyclotron radius. The terms which arise from light-hole intermediate states are approximately a factor of 2 further removed from resonance and have not been included above.

It is interesting to note that the $(+,z)$ cross section [second term in Eq. (1)] is smaller than the $(z,-)$ by a factor of 0.73 (the more detailed numerical calculation discussed above gives a value of 0.78 for the ratio of the polarizations for a photon energy near the band gap). In a nonresonant case the two polarization components are approximately equal for small magnetic fields since the light-hole intermediate-state contributions to the cross section are then comparable to the heavy-hole contributions. At high magnetic fields there is another mechanism which gives rise to a difference between the two polarizations. This is the mixing of conduction- and valence-band states which give rise to the terms in a, b, and A in Eq. (1). Note that there are no additional polarization selection rules that arise when wave-function mixing is included. This is contrary to the results of Wright, Kelley, and Groves.[2] However, it can be shown to hold true even when including all of the intermediate states and also within the more refined band-model calculation that they performed.

The polarization selection rules in Eq. (1) do not imply that one of the photons must be propagating along the field; rather, they imply only that one photon must have a component of polarization along the field and the other a component at right angles to the field. For example, (z,x) scattering where both photons are propagating normal to the magnetic field is included in the $(z,-)$ scattering polarization selection rule.

The polarization data shown in Fig. 1 are in good agreement with the theoretical selection rules contained in Eq. (1). The signal observed in the top trace of Fig. 1 results from the $(z,-)$ term in the cross-section expression of Eq. (1), while the bottom traces indicate that scattering selection rules of the form $(x,\pm)$ and $(\pm,\pm)$ are absent. The comparison between theory and experiment for all possible geometries is summarized in Table I. As a result of the variation in the collection optics for different directions of propagation of the scattered light, the results within each set of data delineated by the double lines are normalized to the maximum theoretical value of the allowed polarization within the set, and no comparison should be made between these sets. Because the optic axis of the sapphire crystal used as a $\frac{1}{4}$-wave plate was only known to within a $\pi/2$ rotation, an experimental assignment of the two measured circular polarization components to right and left circular polarization cannot be made. The agreement between theory and experiment is quite good. The slight depolarization measured can be attributed, at least partially, to the effects of the collection optics. This agreement is in contrast to the recently reported measurements of Patel and Yang[6] of the polarization selection rules of spin-flip Raman scattering using a 10.6-μm laser where almost total depolarization was found.

The resonance enhancement of the spontaneous

TABLE I. Polarization selection rules for spin-flip Raman scattering —comparison of theory and experiment. The experimental values within each set of double lines are normalized to the maximum theoretical value within that set. $n = 1\times10^{16}$ cm^{-3}, $H = 35$ kG, and $T \sim 30$°K.

			INCIDENT PHOTONS					
			$\vec{k}_i \perp \vec{H}$				$\vec{k}_i \parallel \vec{H}$	
			$\vec{E}_i \parallel \vec{H}$		$\vec{E}_i \perp \vec{H}$		$\vec{E}_i = \frac{1}{\sqrt{2}}(\vec{E}_{i+} + \vec{E}_{i-})$	
			Experiment	Theory	Experiment	Theory	Experiment	Theory
SCATTERED PHOTONS	$\vec{k}_o \perp \vec{H}$	$\vec{E}_o \parallel \vec{H}$	0.06	0.0	0.69	0.78	0.78	0.78
		$\vec{E}_o \perp \vec{H}$	1.0	1.0	0.12	0.0	0.07	0.0
	$\vec{k}_o \parallel \vec{H}$	$\vec{E}_{o-}$	1.0	1.0	0.04	0.0	<0.1	0.0
		$\vec{E}_{o+}$	0.02	0.0	0.04	0.0	<0.1	0.0

spin-flip Raman scattering cross section as the input photon energy approaches the InSb band-gap energy was studied experimentally by varying the input laser photon energy. The incident laser beam was directed across $\vec{H}$ and polarized along $\vec{H}$; the scattered light was collected along the magnetic field direction. Although the normal modes of the scattered light are circularly polarized in this geometry (see Table I), only one linear polarization component of the scattered light was collected. This was done so that the data could be corrected for the spectrometer wavelength response which could only be measured using linearly polarized light. Changing the wavelength of the CO laser by tilting the cavity grating resulted in slight changes in the directional characteristics of the laser beam and in the laser mode pattern; the optical alignment was, therefore, readjusted for each measurement. These alignment variations were the dominant source of error, about 10–15%, in measuring the magnitude of the received signal. The laser power was continuously monitored, and the experimental results were normalized to a constant laser power. The system was also flushed with dry nitrogen to eliminate atmospheric absorption effects.

Because the experimental measurements included photon energies very close to the band-gap energy, the data were corrected for sample absorption. This was evaluated by measuring the sample transmission at the same magnetic field (40 kG) as the measurement of the resonance enhancement.

The relative integrated scattering cross section, corrected for both sample absorption and system wavelength response, is shown in Fig. 2 for a magnetic field of 40 kG. The average laser power was kept below 250 mW at all times in these measurements to avoid sample heating effects.

Also shown in Fig. 2 is a theoretical resonance enhancement curve based on the numerical cross-section calculation discussed above. The band parameters used in this numerical computation were those of Pidgeon and Brown,[1] which were obtained from an analysis of interband absorption data. Any reasonable adjustment of these parameters would have only a small effect on the computed resonance curve. Thus, we have used only one adjustable parameter in the fit between theory and experiment. This is an overall multiplicative constant as only the relative, not the absolute, cross section was measured. This parameter was chosen to give a good fit at the lower energies where the data were less sensitive to corrections for sample absorption. The form of the resonance enhancement can also be seen in Eq. (1) with the proviso that nonparabolicity effects must be included in the evaluation of the conduction-band energies.

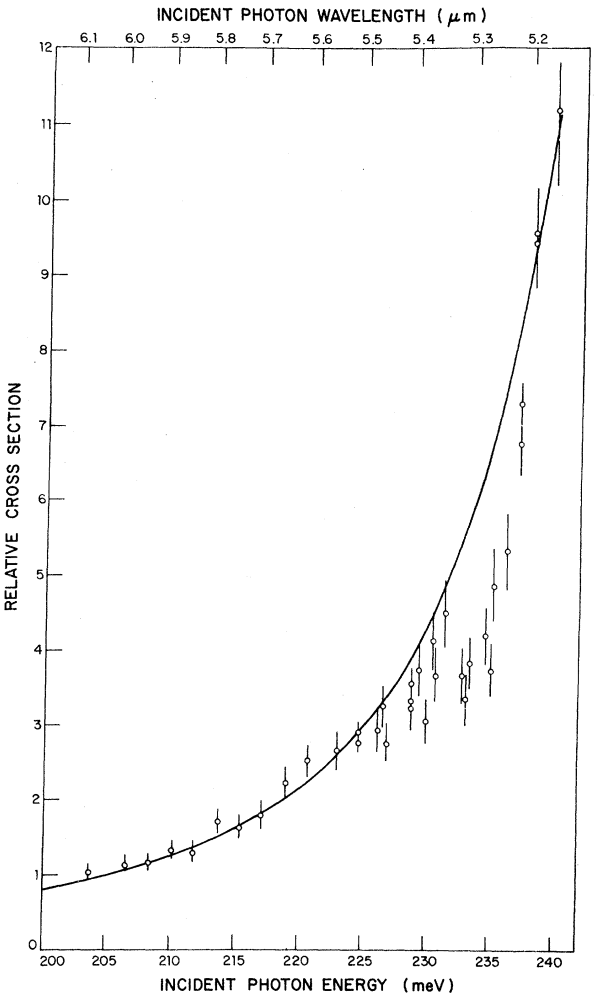

FIG. 2. Resonance enhancement of spontaneous spin-flip Raman scattering as a function of input photon energy. $n = 1\times10^{16}$ cm^{-3}, $H = 40$ kG, and $T \sim 30$°K.

There is qualitatively good agreement between theory and experiment for a variation of over an order of magnitude in the relative cross section. There is some structure in the experimental results for input photon energies around 235 meV that is not predicted by the theory. This might arise from Raman processes that proceed via an impurity level as the intermediate state. There is an absorption due to a Zn acceptor level which starts at about 229 meV at $H = 0$. This acceptor level has an absorption threshold of about 236 meV at a magnetic field of 40 kG where these

measurements were made.[7] The levels associated with this absorption must be included in the sum over intermediate states in evaluating the cross section; because of possible interference effects, the result of including these states in the theory is not immediately evident. Further study is necessary to resolve this point.

We wish to thank D. J. Wells for expert assistance, K. Nearen for cutting, and W. Laswell for polishing the samples.

*Work sponsored by the U. S. Air Force.

[1]C. R. Pidgeon and R. N. Brown, Phys. Rev. 146, 575 (1966).

[2]G. B. Wright, P. L. Kelley, and S. H. Groves, in *Light Scattering Spectra of Solids*, edited by G. B. Wright (Springer-Verlag, New York, 1969), pp. 335–343.

[3]A more detailed discussion of both of these cross-section calculations as well as the experimental results is contained in S. R. J. Brueck, Ph.D. thesis, Massachusetts Institute of Technology, 1971 (unpublished).

[4]Y. Yafet, Phys. Rev. 152, 858 (1966).

[5]V. P. Makharov, Zh. Eksp. Teor. Fiz. 55, 704 (1968) [Sov. Phys. JETP 28, 336 (1969)].

[6]C. K. N. Patel and K. H. Yang, Appl. Phys. Lett. 18, 491 (1971).

[7]A. Mooradian and H. Y. Fan, Phys. Rev. 148, 873 (1966).

Rotationally Invariant Theory of Spin-Phonon Interactions in Paramagnets

R. L. Melcher
IBM Thomas J. Watson Research Center, Yorktown Heights, New York 10598
(Received 1 December 1971)

We propose a theory of spin-phonon interactions in paramagnetic materials. The theory is based upon the conservation of total, i.e., spin plus lattice, angular momentum. Rotational invariance of the Hamiltonian of the coupled system leads to new contributions to the spin-phonon interaction. These new contributions are determined by the anisotropy of the crystal field acting on the spin system.

Previous treatments of the interaction between spins and phonons in paramagnetic crystals have assumed *a priori* that the spins are coupled to the lattice only via deformations of the latter which can be described by a symmetrical elastic strain tensor e_{ij}.[1] In this paper we require the total Hamiltonian of the coupled spin-lattice system to be consistent with conservation of total angular momentum. This requirement leads to additional contributions to the spin-phonon interaction which have been previously ignored and which contribute antisymmetrical components to the stress tensor.

Total angular momentum of a closed system is conserved if the Hamiltonian $\mathcal{H}$ is invariant to arbitrary rigid rotations of the system. Consider a paramagnetic spin $\vec{S}$ in an otherwise diamagnetic host lattice in the presence of an external field $\vec{H}$. Angular-momentum conservation requires that the Hamiltonian of this system is invariant to rigid rotations of the spin, the lattice, and the field together. We assume that the Hamiltonian $\mathcal{H}$ describing the potential or stored energy is a function of the following variables:

$$\mathcal{H}=\mathcal{H}(S_i, H_i, \partial x_i/\partial X_j). \tag{1}$$

Here, the spatial coordinate $\vec{x}$ is the instantaneous position of the ion and the material coordinate $\vec{X}$ is its position in the undeformed lattice. By assuming the lattice energy to be determined solely by the deformation gradients $\partial x_i/\partial X_j$ and hence independent of the displacements $\vec{u}=\vec{x}-\vec{X}$, $\mathcal{H}$ automatically has translational invariance. As written in Eq. (1), $\mathcal{H}$ is a function of the components of five vectors: $\vec{S}$, $\vec{H}$, and $\partial\vec{x}/\partial X_j$, $j=1,2,3$. Such functions have complete rotational invariance if they can be expressed as functions of scalar invariants.[2] We choose the following complete but not unique set of invariants:

$$S_k^*=S_iR_{ik}, \tag{2a}$$

$$H_k^*=H_iR_{ik}, \tag{2b}$$

$$E_{kl}=\tfrac{1}{2}[(\partial x_i/\partial X_k)\partial x_i/\partial X_l-\delta_{kl}]. \tag{2c}$$

Here, R_{ik} is the finite rotation tensor and E_{kl} the finite strain tensor of the classical theory of elasticity. The invariants S_k^* and H_k^* are the components of spin and field on having been rigidly rotated by R_{ik}.[3] The above set of scalar invariants is complete only to the extent that parity is conserved, i.e., that $\mathcal{H}$ is invariant to spatial inversion, $\vec{x}\rightarrow-\vec{x}$.[2] The rotationally invariant